

Shear-Wave Velocity Structure underneath the City of Padang, Indonesia

Xiaohan Han & Kusnowidjaja Megawati

Earth Observatory of Singapore, Nanyang Technological University, Singapore

Hiroaki Yamanaka

Tokyo Institute of Technology, Japan



SUMMARY

Padang is in vicinity to the Sumatran fault zone, and faces great earthquake hazards. To assess its seismic hazard, a 3D shear-wave velocity structure was to be constructed for the city. We conducted 42 pairs of microtremor array measurements to understand the shear-wave velocity structure. Surface waves recorded were analyzed using the spectral autocorrelation (SAPC) method and the frequency-wavenumber (F-k) method. Our study indicates that soft soil covers the top 30 meters of the ground of the metropolitan Padang. The soil in the coastal regions has $V_{s,30}$ ranging between 140 and 230 m/s. The soil east Padang has $V_{s,30}$ over 300 m/s. Soft soil layers with velocity lower than 350 m/s are about 25 meters to 80 meters thick. Large arrays results were able to estimate deeper sedimentary rock structure. Generally, it takes 200 to 300 meters to reach a layer with shear-wave velocity of 1 km/s.

Keywords: microtremor, Padang, spectral autocorrelation, frequency-wavenumber

1. INTRODUCTION

During active periods of the Sumatran megathrust, cities located in vicinity of the west Sumatran coast, such as Padang, the second largest city on Sumatra Island, face extremely high seismic hazards. The cycle of the Sumatran megathrust, formed by the Eurasian plate subducting under the Indo-Australian plate, has been established to be around 200 years (Sieh et al, 2007), with the most recent cycle starting with the Aceh earthquake on 24th December 2004. The strain between plates is released patch by patch from north to south and this process has initiated several giant earthquakes from 2005 to 2012. The last patch beneath the Mentawai is expected rupture in the near future (Figure 1.1). If this happens, Padang will be at great risk due to its close distance. Many studies have been carried out to investigate the faulting mechanisms of the Mentawai patch and predict the magnitude the earthquake (Natawidjadja and Sieh, 2006). To prepare for natural disaster, the assessment of the seismic risk is crucial. The risk depends on, in addition to source, the paths of seismic wave transmission, as well as the socio-economic conditions of the site. The path of seismic wave transmission could be estimated by establishing regional crustal structures. The local site conditions need to be determined to predict soil responses and calculate ground motions.

Padang sits on the west coast of Sumatra, and most of the city is located between the river mouths of the Arau River and the Kuranji River. The soil profile beneath Padang is mainly composed of unconsolidated Holocene-Pleistocene quaternary rocks (Crow and Barber, 2005). The materials covering the unconsolidated bedrock vary from the western coastal region to the eastern hilly region. The top layer soil along the coastal plains is the sea sediment while beyond the plains is volcanic sediment (Crow and Barber, 2005). As the soft sediment would amplify the seismic waves by many folds, the effects of site conditions should not be underestimated. Many researchers have looked at the site responses in relation to site characteristics, such as the shear wave velocity averaged over the top 30m of soil ($V_{s,30}$). The $V_{s,30}$ value is an important parameter for evaluating dynamic behaviour of soil and categorizing site conditions. However, only a few preliminary $V_{s,30}$ maps have been plotted

based on geographical information. Peterson et al (2007) produced a map based on geological maps published in the mid 1970s by the Indonesia Geological Survey, by directly matching the soil categories to the generalised geologic units. For example, D category was assigned to quaternary alluvium and BC to quaternary-tertiary volcanic rocks. The source of the geological map gives poor and indiscriminate projections on the soil structures beneath the city. Therefore, the accuracy of the $V_{s,30}$ map might be limited by the geologic units. Allen and Wald (2009) produced $V_{s,30}$ data worldwide by relating the shear wave velocity value to the topography slope. Stronger soil strength could reside on a steep slope because of the strong bonding between the soil materials. And soil materials on a flatter slope indicate finer and softer soil. However, the general relationship was obtained from locations with abundant data, such as the US and Taiwan. The relationship need to be tested at interesting sites other than these places.

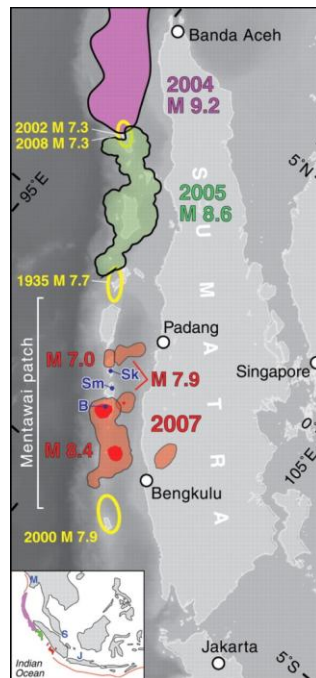


Figure 1.1 Recent ruptures on the Sumatran fault (Sieh *et al*, 2007).

The aim of our research is to use microtremor survey method (MSM) to construct the 3-D shear wave velocity structures of Padang. Developed by Hiroshi Okada (2003), MSM is a convenient tool for estimating the shear wave velocity structures in densely built urban cities due to its low labour and operation cost. Under the fundamental assumption of surface waves as stochastic waves, MSM differs from conventional seismic methods by its utilization of natural random seismic noises and identification of spatial stability of dispersion. The dispersion relationship is used for inversion of subsurface structure (Horike, 1985). MSM detects the soil micro tremors below the observation network and records them in the seismometers. The horizontal and vertical dispersion relationship of micro tremor waves in different recording stations could be determined using analytical methods such as the frequency wave number method (Aki, 1957; Capon 1969). MSM can capture longer wave periods by enlarging the network size to detect the dispersion from deeper soil structure. Based on the shear wave velocity structure obtained, the site conditions in Padang could be determined for further seismic risk assessment.

2. MICROTREMOR SURVEY AND INTERPRETATION METHOD

A total of 22 groups of small arrays and 16 large arrays were carried out in the city of Padang in the daytime between 16th and 26th of August, 2010 (Figure 2.1). The HKS 9550 recorder was used with the sampling frequency set at 100 samples per second, together with a VSE-15D6 velocity-meter with

flat amplitude from 0.1 to 50 Hz and a GPS receiver to locate the real spatial position of the recording site and synchronize the recording time.

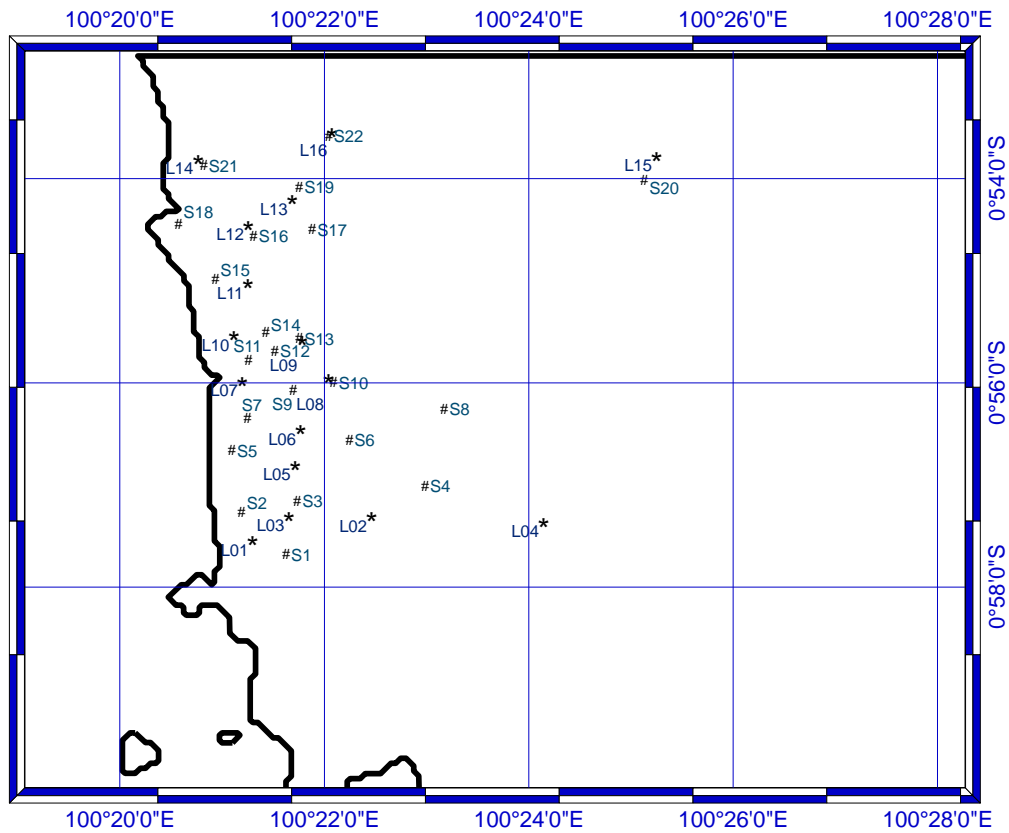


Figure 2.1 Locations of microtremor array measurements

The selection of microtremor survey sites were considered based on the availability of open space for the desired configuration. Google Earth was used as a reference map for current land uses in Padang. The locations of survey sites were selected and labelled in scale on the Google Earth. The real measurement sites differed from the planned location when the surface condition was not favourable. On an open field, we located our sensors over a ceramic tile on concrete grounds, asphalt road or soccer fields.

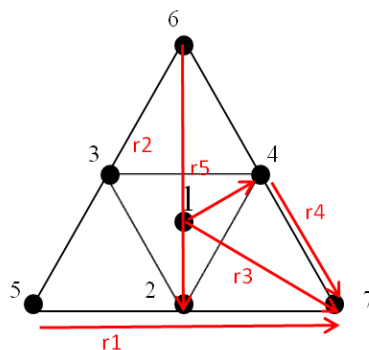


Figure 2.2 Configuration of array measurement

We carried out the measurements with seven sensors in a configuration of an equilateral triangular shape. Three equally spaced sensors were the vertex of the triangle (sensor Number 5, 6 and 7, see

Figure 2.2) and three sensors were on the middle of the triangle sides (sensor Number 2, 3 and 4). The last sensor (sensor Number 1) was in the middle of the triangle. This configuration will give five combinations of distances (r_1 to r_5) between 2 pairs of sensor stations.

The size of small and extra-small array was determined on site to utilise the open space available. Different array combinations were used such as 5 meters with 20 meters, as well as 10 meters with 40 meters. The positions of the seven stations were located with GPS and noted in the recording log. The local time of recorders is synchronized with GPS. Recordings of microtremor on each sensor lasted for about 30 minutes. Surface wavelets resembling each other were detected and caught in the sensors. The spatial autocorrelation (SPAC) method (Aki, 1957) was used for analyzing the wavelets from small arrays. Frequency-wave number (F-k) analysis of microtremor (Capon, 1969) was used for detecting the dominant surface waves that have the highest power for medium and large arrays (array size larger than 200 meters).

The SPAC method calculates the self coherence coefficient of wavelets for a separation of time as a dispersion function of frequency via the Bessel's function (Figure 2.3 (i)). For a 30-minute recording, more than 10 segments of recording of the size of 8092 samplings can be produced for spectral analysis. For each duration segment, the spatial autocorrelation coefficient is calculated for a given period of wavelets for one array size (Figure 2.3 (i (a))). This coefficient is the azimuthal average of the coherency of the records at the ends of each array configuration for a period T . We put the correlation coefficients of five array sizes in the plot of this given period and fit the coefficients with the Bessel's function by finding a proper value of phase velocity (i (b)). The phase velocity is calculated with Equation 2.1.

$$c(T) = \frac{2\pi r_0}{T_0 x_0} \quad (2.1)$$

x_0 is the distance as a variable in the Bessel function of the first kind of 0th order. The averaged value of phase velocity is calculated from all the segments with a standard deviation (Figure 2.3 (i (c))). This phase velocity is a reflection on the subsurface structures, whose properties are to be determined through an inversion process.

While the frequency-wave number (F-k) method will calculate the power and cross spectra of microtremor collectively as F-K spectrum. The spectrum is used to identify phase velocities and azimuths from the dominant surface wave. Given a frequency T_0 , the f-k spectra gives the wave numbers of the dominant waves (K_{x_0}, K_{y_0}), and the phase velocity c_0 is calculated from Equation 2.2.

$$c_0 = \frac{2\pi}{T_0 \sqrt{k_{x_0}^2 + k_{y_0}^2}} \quad (2.2)$$

The phase velocity plotting starts with the smaller array from broader wave number range to a narrower wave number range. The f-k spectrum of an array catches a higher phase velocity at a longer period and a continuous increase of phase velocity should be observed. Confined in a proper wave number range, one highest phase velocity could be noticed at a certain period than other periods. Therefore, the trials of picking a proper range to catch his highest velocity were done a few times (Figure 2.3 (ii (b))).

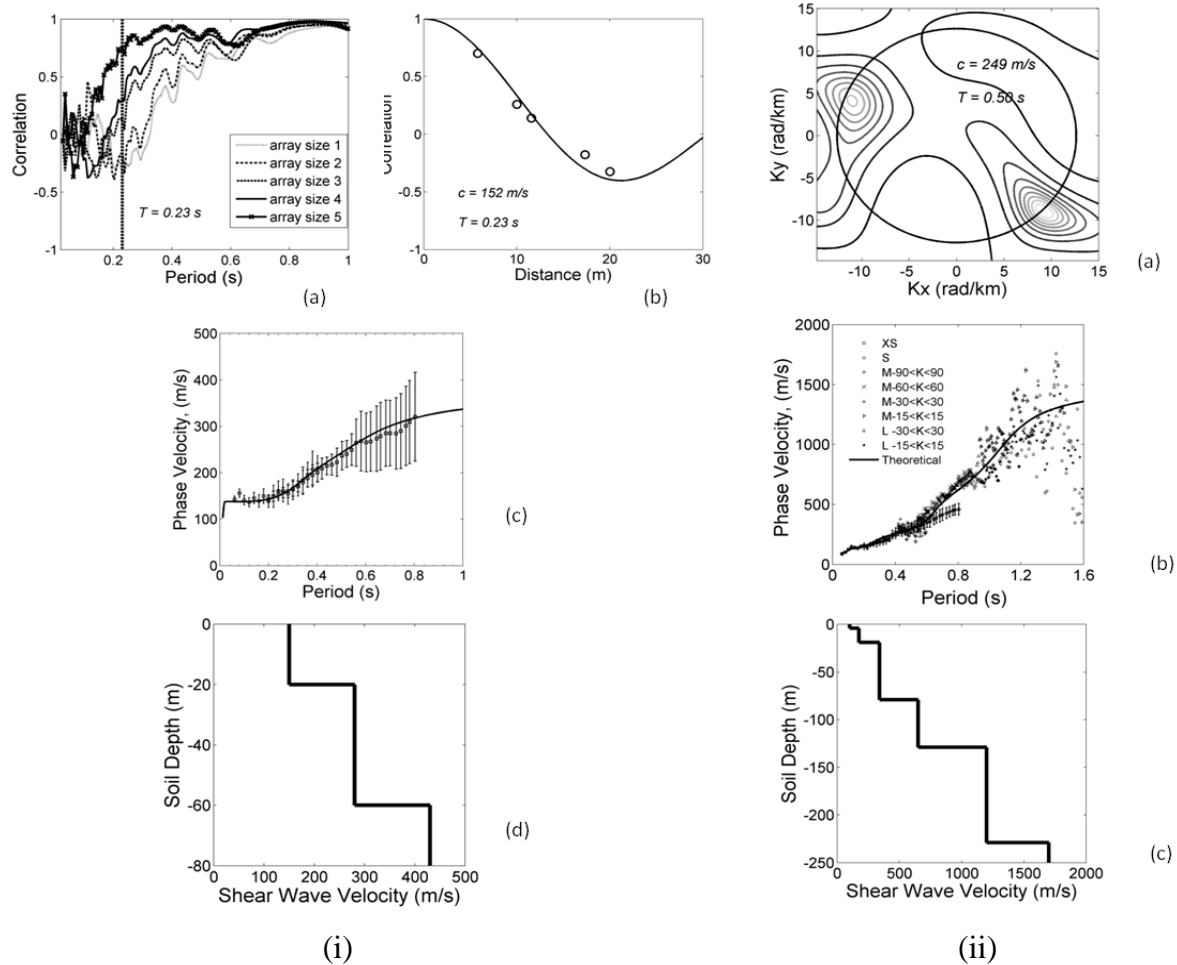


Figure 2.3 SPAC and F-k methods of analysing microtremor results.

An inversion of soil structure is carried out to fit the observed phase velocity. For soil with parallel and isotropic layers, a theoretical value of the phase velocity is expressed as a function of depth (H), soil density (ρ), s-wave velocity (V_s), and p-wave velocity (V_p) (Horike, 1985). We assumed that the soil beneath Padang is clearly layered horizontally and homogenous within each layer. The soil properties can be reduced to two parameters by relating P-wave velocity and density to the shear wave velocity. We used $V_p = 1.732V_s$ and $\rho = 1.8$ to 2.4 ton per cubic meter. Therefore, we are able to build models of soil structures and calculate their theoretical phase velocity, which will be used to fit with phase velocity obtained in the observations (Figure 2.3 (i(d), ii(d))). The inversions that produced the most number of fits to the mean values of the observed phase velocity are accepted and improved by careful iterations. Four to five layers are used for the modelling of small arrays and up to eight layers for the large arrays where the layers can be separately identified from the dispersion curve. The last layer was considered to have an infinite thickness. As medium and large arrays could not resolve the shallow soil structures, the shallow structure inverted from small array on the nearby sites was used to provide a guide for the inversion of deeper soil. The inversion process of finding the best fit soil structure was carried out three times to reduce bias. Averaged V_s for the top 30 meters is calculated from the inverted modelled structure to give the soil strength indicator $V_{s,30}$.

3. RESULTS

3.1 V_s , 30 Map

Twenty two observations in Padang were able to capture the dispersion correlations of the surface waves between channels and identify a characteristic phase velocity. We calculated shear wave velocity for the top 30 meters using phase velocities from small arrays (5 meters to 40 meters). The location of these sites and their Vs,30 values are listed in Table 3.1. The value of calculated Vs for each small array site and the interpolation map obtained using the Kriging technique is shown in the Figure 3.1.

Table 3.1 Location Of Measurement Sites And Vs,30 Values

Site Number	Vs, 30 (m/s)	Latitude	Longitude	Site Number	Vs, 30 (m/s)	Latitude	Longitude
01	199	-0.96138	100.36061	12	181	-0.92824	100.35877
02	204	-0.95448	100.35333	13	183	-0.92618	100.36271
03	218	-0.95266	100.36237	14	184	-0.92518	100.35726
04	336	-0.95024	100.38323	15	170	-0.91649	100.34904
05	177	-0.94441	100.35174	16	165	-0.90950	100.35528
06	158	-0.94274	100.37090	17	190	-0.90844	100.36483
07	185	-0.93928	100.35427	18	196	-0.90749	100.34305
08	308	-0.93767	100.38635	19	200	-0.90147	100.36271
09	195	-0.93461	100.36168	20	212	-0.90041	100.41897
10	200	-0.93336	100.36833	21	156	-0.89796	100.34712
11	170	-0.92971	100.35445	22	205	-0.89311	100.36751

From the interpolation results, we found there is a tendency for soil to become harder towards the east and towards the south, where the hills are located. Vs,30 values close to the coast in the western part of the sediment plain basin are between 150 m/s to 180 m/s. The lower Vs,30 value can be resulted from flushing and depositing of the rivers and sea due to its location on the estuary and vicinity to the coast. Vs,30 values near the eastern boundary of the plain are beyond 180 m/s as the soil become thinner towards the foot hills and the site becomes more rocky.

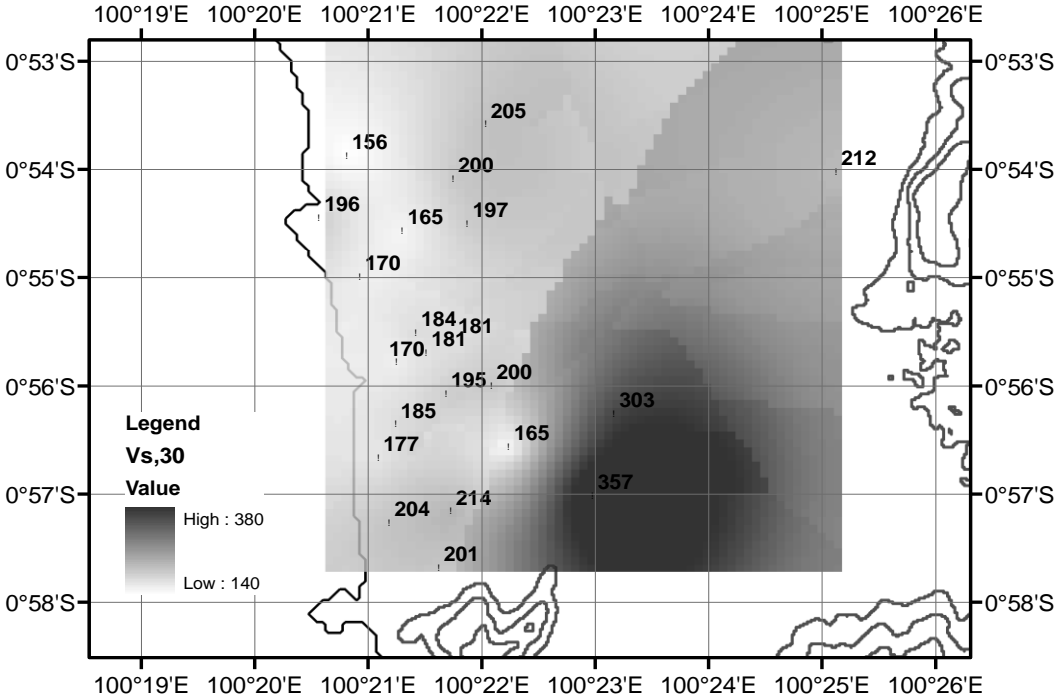


Figure 3.1 Map of the interpolated Vs,30 values

According to the International Building Code (IBC 2006), soil with Vs,30 between 180 m/s to 360 m/s is classified as stiff soil in category D, which has been credited indiscriminately to the plain basin in

Padang in the Seismic Design Code of Indonesian National Standard. Allen and Wald (2009) gave the same results too, in their $V_{s,30}$ map based on Shuttle Radar Topography Mission (SRTM) 30 arcsec digital elevation models (DEMs). However, the results of microtremor survey show that there is soft soil near the coastal sites with $V_{s,30}$ values lower than 180m/s belonging to category E. For easy visualization, we produced a plot of newly classified map shown in Figure 3.2.

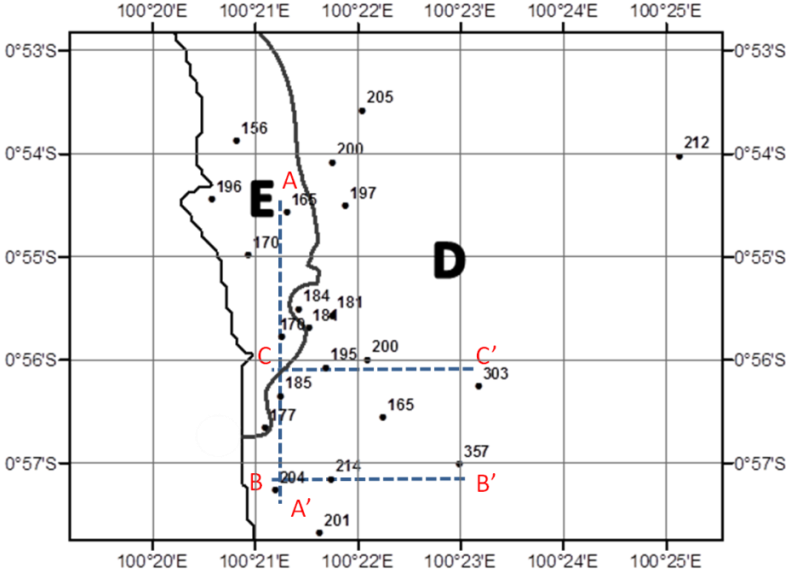


Figure 3.2 Site classification based on microtremor results

Studies correlating the site amplification factors to site class show that amplification factor will increase when $V_{s,30}$ is lower. According to the studies done for NEHRP, the amplification of soil in Class E is 1.6 folds to the value of soil in Class D for long period of accelerations, and the ratio of amplification of E and D class is between 0.9 to 1.6 times for short period of accelerations, depending on the acceleration value. Therefore, coastal site will experience larger amplification of ground motion due to its site condition and impose higher demand on the structures compared to the site conditions in south and east.

3.2 Shallow Soil Structures Obtained from Small Arrays

To check the spatial variations of the soil characteristics, we plotted the soil profile on three cross-sections (Figure 3.3 to Figure 3.5). One cross section is along the coastline and about 1 km from the shore. This line passes through the most populated part of the city (A-A'). The array numbers from south to north are 2, 5, 7, 11, 14 and 16. The inverted soil structures show similar V_s between the depths of 5 meters to 25 meters (Figure 3.3 (a)). The depths reaching $V_s = 200\text{m/s}$ and 400m/s are shown as dotted lines in Figure 3.3 (b). A rather homogenous soil profile could be observed with sediment depth a little thicker in north than in south. The southern part of Padang is hilly, which results in a shallower depth of soft soil. Another two cross-sections pass through central and south Padang from east to west. The array numbers on cross-section B-B' are 2, 3 and 4 (Figure 3.4); the array numbers on cross-section C-C' are 7, 9, 10 and 8 (Figure 3.5).

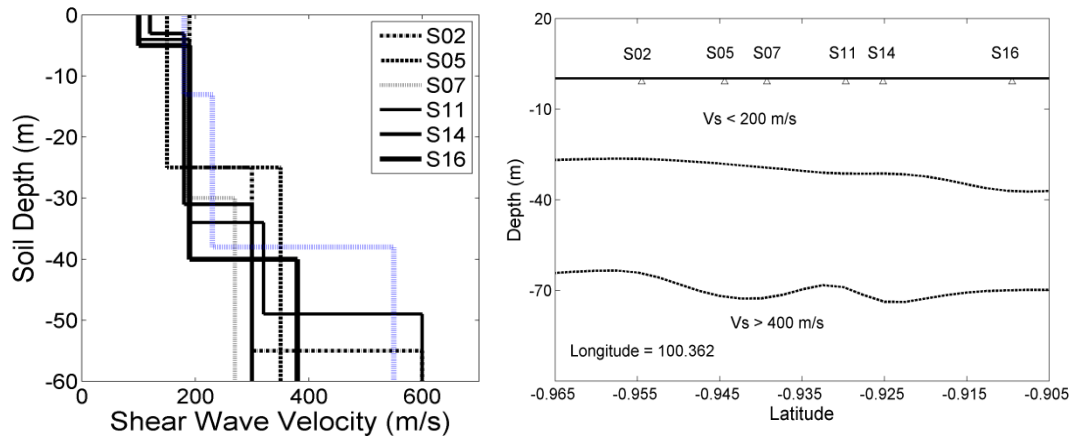


Figure 3.3 Soil structure (a) and sub-surface profile (b) along cross-section A-A'

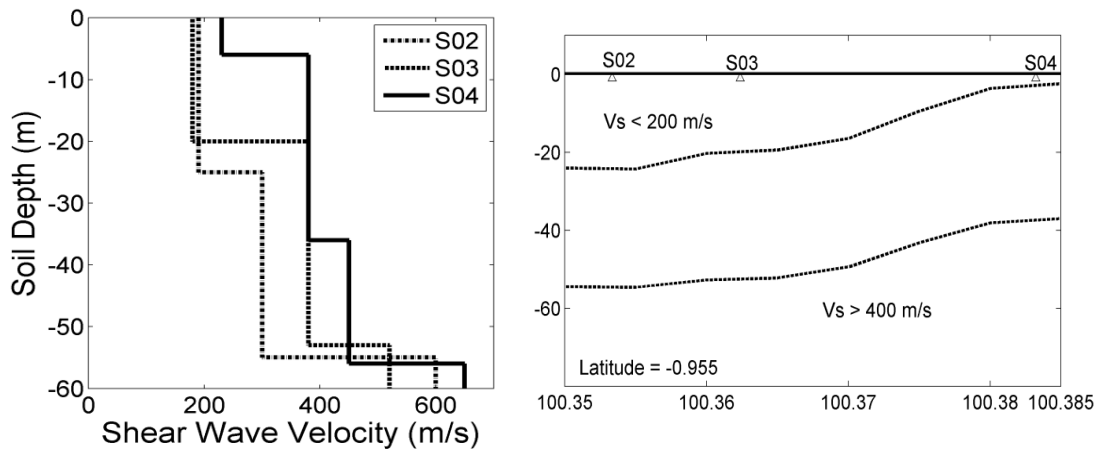


Figure 3.4 Soil structure (a) and sub-surface profile (b) along cross-section B-B'

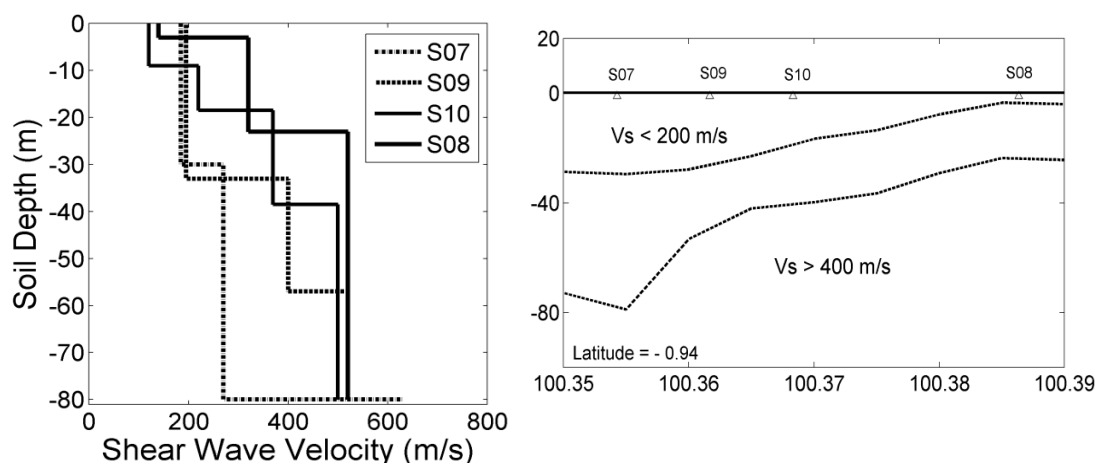


Figure 3.5 Soil structure (a) and sub-surface profile (b) along cross-section C-C'

The variations of soil structures can be clearly observed. The depth of soil deposit decreases gradually from around 30 meters near the coast to about 5 meters near the western hilly zone. The depth to

engineering bedrock ($V_s > 400\text{m/s}$) is shallower towards the west, showing similar trend as the deposit depth. It can be accepted that the soil deposit is thinner to the east because of the volcanic sediments in the east and the rivers join the sea in the west. The sediment depth is thinner in the south than in the north, because of the presence of southern hills; this implies a lower shear wave velocity in north Padang. Generally speaking, the soil profile is rather continuous and follows a trend. Therefore, the interpolated value of shear wave velocities based on microtremor results should be promising and reasonable.

3.3 Bedrock Depth Obtained from Medium and Large Arrays

The length of an array is approximately proportional to the depth of the deepest penetration. To verify the penetration depth and find soil structures in deep soil, we analyzed the dispersion of longer wave periods and compared the depth of hard rock at different locations. We found that large arrays (200 meters to 1000 meters) gave a clear and consistent dispersion relationship of the dominant waves with periods up to 2 seconds. Furthermore, the array could reach a rock layer with $V_s > 1000\text{ m/s}$. Western plain reaches hard rock at depth at approximately 200 meters to 350 meters. The north part of the eastern plain reaches hard rock at depth around 200 meters (Figure 3.6).

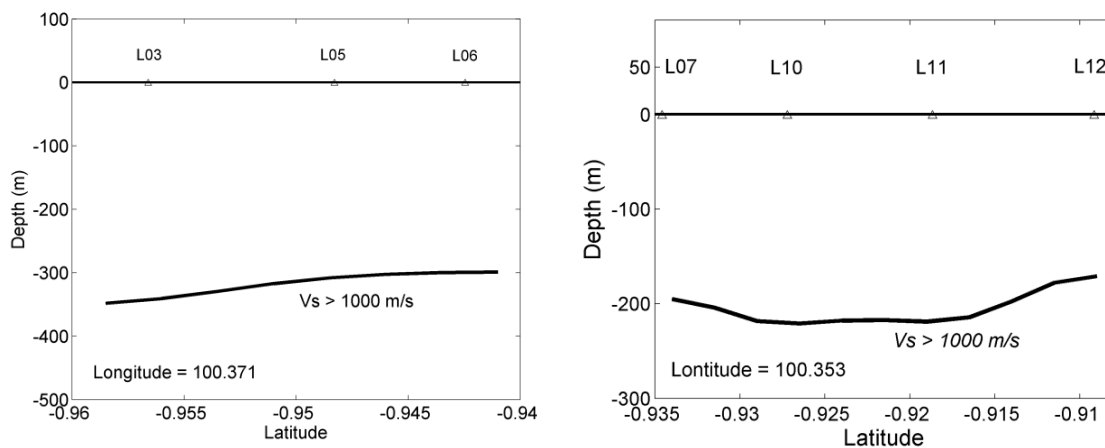


Figure 3.6 Depth of rock bed ($V_s > 1000\text{ m/s}$) below the stations along the shoreline.

Soil generally becomes stiffer as the depth increases. Shallower depth to the hard rock in southeastern Padang explains the observation of higher V_s values in this area. In west Padang, the soil structure is predictable and has less variation inside the plain. While towards the east, the soil becomes stiffer and the trend is revealed by the dispersion detected in a large array.

4. CONCLUSIONS

The microtremor array method was used to study the V_s profile in Padang. The dispersion of surface waves and Rayleigh wave has been captured with the SPAC method for small array size and f-k method for large array size. The three dimensional V_s structure is estimated, inverted from which the theoretical phase velocity is modeled to fit the observed phase velocity. Based on the results, we concluded that the proposed method has produced a three dimensional V_s structure down to bedrock. Generally, the V_s value increases from the west to the east, from north to the south. The variation confirms with the geology of the area. The dispersion of surface waves was clearly recorded and able to produce reasonably reliable values of shear wave velocity. Based on the details of the inversion soil structure, the site amplification and responses could be calculated within a reasonable range. More recording could be carried out in Padang, to produce a more detailed profile in Padang to identify hidden soft-strength land in east Padang.

AKCNOWLEDGEMENT

The authors would like to thank Dr. Meya Yanger Walling and Mr Zhu Cheng (Earth Observatory of Singapore, Singapore) for their cooperation with the site measurements. Financial support provided by the Earth Observatory of Singapore, Singapore.

REFERENCES

- Allen, T. I., and Wald, D. J. (2007). Topographic Slope as a Proxy for Seismic Site Conditions ($V_s,30$) and Amplification around the Globe. *U.S. Geological Survey Open File Report* **2007-1357**, 69.
- Aki, K. (1957) Space and time spectra of stationary stochastic waves with special reference to microtremors, *Bulletin of the Earthquake Research Institute* **35**, 415-456.
- Barber, A.J., and Crow, M.J. (2005). Sumatra: Geology, Resources and Tectonic Evolution. Geological Society, London, Memoirs.
- Capon, J. (1969) High-resolution frequency-wavenumber spectrum analysis. *Geophysics* **34**(1), 21-38.
- Horiike, M. (1985). Inversion of phase velocity of long-period microtremors to the S-wave-velocity structure down to the basement in urbanized area. *Journal of Physics of the Earth* **33**, 59-96.
- Natawidjadja, D.H., Sieh, K., Chlieh, M., et al. (2006) Source parameters of the great Sumatran megathrust earthquakes of 1797 and 1833 inferred from coral microatolls. *Journal of Geophysical Research* **111**, B06403, doi 10.1029/2005JB004025.
- Natawidjadja, D.H., Sieh, K., Chlieh, M., et al. (2007) Interseismic deformation above the Sunda Megathrust recorded in coral microatolls of the Mentawai island, West Sumatra. *Journal of Geophysical Research* **112**, B02404, doi 10.1029/2006JB004450.
- Okada, H. (2003). The microtremor survey method. Geophysical Monograph Series, Society of Exploration Geophysicists, Tulsa, OK.
- Pacific Engineering and Analysis. (2005). NEHRP site class ($V_s,30$) amplification factors from site response simulations. Pacific Engineering and Analysis.
- Peterson, M., Harmsen, S., et al (2007) Documentation for the Southeast Asia Seismic Hazard Maps, *U.S. Geological Survey Open-File Report*.
- Seismic Design Code of Indonesian National Standard (SNI-1726-2002). (2002). Indonesian National Standardization Agency.
- Sieh, K., Natawidjadja, D.H., Meltzner, A.J., et al. (2008). Earthquake supercycles inferred from sea-level changes recorded in the corals of West Sumatra. *Science* **322**, 1674.
- The International Building Code. (2006). Chapter **16**, Structural Design, Section **1613**, Earthquake Loads.